Accepted: 5 February 2018

DOI: 10.1111/epi.14037

FULL-LENGTH ORIGINAL RESEARCH

Epilepsia®

A comprehensive approach to identifying repurposed drugs to treat *SCN8A* epilepsy

Talia A. Atkin[1] | Chani M. Maher[1] | Aaron C. Gerlach[2] | Bryant C. Gay[1] | Brett M. Antonio[2] | Sonia C. Santos[2] | Karen M. Padilla[2] | JulieAnn Rader[1] | Douglas S. Krafte[2] | Matthew A. Fox[1] | Gregory R. Stewart[1] | Slavé Petrovski[1,3] | Orrin Devinsky[1,4] | Matthew Might[1,5] | Steven Petrou[1,3] | David B. Goldstein[1,6]

[1]Pairnomix, Plymouth, MN, USA

[2]Icagen, Durham, NC, USA

[3]Florey Institute for Neuroscience and Mental Health and Department of Medicine, Royal Melbourne Hospital, University of Melbourne, Parkville, Victoria, Australia

[4]Department of Neurology, New York University Medical Center, New York, NY, USA

[5]University of Alabama at Birmingham, Birmingham, AL, USA

[6]Institute for Genomic Medicine, Columbia University Medical Center, New York, NY, USA

Correspondence
David B. Goldstein, Institute for Genomic Medicine, Columbia University, New York, NY, USA.
Emails: dgoldstein@pairnomix.com; dbgoldstein@columbia.edu

Funding information
The work was funded by Pairnomix.

Summary

Objective: Many previous studies of drug repurposing have relied on literature review followed by evaluation of a limited number of candidate compounds. Here, we demonstrate the feasibility of a more comprehensive approach using high-throughput screening to identify inhibitors of a gain-of-function mutation in the *SCN8A* gene associated with severe pediatric epilepsy.

Methods: We developed cellular models expressing wild-type or an R1872Q mutation in the $Na_v1.6$ sodium channel encoded by *SCN8A*. Voltage clamp experiments in HEK-293 cells expressing the *SCN8A* R1872Q mutation demonstrated a leftward shift in sodium channel activation as well as delayed inactivation; both changes are consistent with a gain-of-function mutation. We next developed a fluorescence-based, sodium flux assay and used it to assess an extensive library of approved drugs, including a panel of antiepileptic drugs, for inhibitory activity in the mutated cell line. Lead candidates were evaluated in follow-on studies to generate concentration-response curves for inhibiting sodium influx. Select compounds of clinical interest were evaluated by electrophysiology to further characterize drug effects on wild-type and mutant sodium channel functions.

Results: The screen identified 90 drugs that significantly inhibited sodium influx in the R1872Q cell line. Four drugs of potential clinical interest—amitriptyline, carvedilol, nilvadipine, and carbamazepine—were further investigated and demonstrated concentration-dependent inhibition of sodium channel currents.

Significance: A comprehensive drug repurposing screen identified potential new candidates for the treatment of epilepsy caused by the R1872Q mutation in the *SCN8A* gene.

KEYWORDS
drug library, epilepsy, precision medicine, repurposed drugs, *SCN8A*

1 | INTRODUCTION

A rare disease is defined by the U.S. Food and Drug Administration (FDA) Orphan Drug Act of 1983 as one affecting <200 000 individuals in the United States. Collectively, however, rare diseases affect >20 million people in the United States, reflecting 6%-7% of the population. The majority of these diseases are genetic, and only about 5% have an FDA-approved treatment.[1] Advances in sequencing technologies have helped to identify a growing number of genes linked to rare diseases, providing insight into the pathoetiologies of these disorders. Recently, there has been interest in developing treatments for genetic epilepsies by targeting underlying mechanisms.[2] Here, we adopt a precision medicine approach to identify potential candidate treatments for a patient with an epileptic encephalopathy caused by a mutation in *SCN8A*.

SCN8A encodes the alpha subunit of the voltage-gated sodium channel, $Na_v1.6$, abundant in the peripheral and central nervous system (CNS), and found predominantly at the nodes of Ranvier.[3] $Na_v1.6$ helps regulate neuronal excitability through its unique location in the distal part of the axon initial segment,[4] its low voltage threshold for activation,[5] and its contribution to resurgent[6] and persistent[7] sodium-derived currents. Mutations in $Na_v1.6$ are estimated to account for 1% of epileptic encephalopathies.[8] The R1872 residue (GenBank NM_014191.3) is the most frequently reported site for disease-causing mutations in *SCN8A*, and cellular models have shown a gain-of-function phenotype caused by variants at this site.[9] We addressed the functional effects of an *SCN8A* de novo mutation where arginine is substituted for glutamine, R1872Q (NM_014191.3:c.5615G>A;p.R1872Q). This mutation was reported to cause a gain-of-function molecular phenotype involving excess sodium influx upon neuronal activation, resulting in hyperexcitability that may contribute to the epileptic encephalopathy clinical phenotype.[9] Therefore, inhibiting excess sodium influx into the cell could have specific therapeutic value by reducing neuronal hyperexcitability caused by this mutation.

We characterized the *SCN8A* R1872Q mutant channel in a stably transfected HEK293 cell line, confirmed the gain-of-function phenotype, and carried out high-throughput drug screening using a fluorescent imaging plate reader (FLIPR) assay. We identified 90 compounds that significantly inhibited sodium influx into the cell from a chemical library of 1320 compounds that included clinically approved drugs and nutritional supplements. Three compounds appear to be promising therapeutic candidates based on their inhibitory activity, brain uptake, and safety profile: carvedilol (beta-blocker used to treat congestive heart failure), amitriptyline (serotonin-norepinephrine reuptake inhibitor antidepressant), and nilvadipine (calcium channel blocker used for hypertension). We confirmed, and further characterized, their inhibitory effects using electrophysiology in an HEK293 cellular model. These findings demonstrate the value of using personalized cellular models of a clinically relevant patient mutation to generate a clinically relevant platform for comprehensive drug repurposing effectiveness screening. This approach is conducive to identifying candidate treatments for patient-specific mutations manifesting as rare diseases, such as the infantile epileptic encephalopathies.

Key Points

- A heterologous in vitro cell model replicated the electrophysiological gain-of-function changes previously described with an *SCN8A* R1872Q pathogenic variant
- A high-throughput screen with a library of approved drugs identified numerous hits with significant inhibitory activity against the R1872Q mutant cell model
- For many of the hit compounds from the library, inhibitory activity at the $Na_v1.6$ sodium channel, or sodium channels in general, had not been previously described
- These findings present new therapeutic options using repurposed drugs for the treatment of epileptic encephalopathy arising from this *SCN8A* mutation
- The results also demonstrate the utility of a comprehensive high-throughput drug screening approach that combines personalized and precision medicine

2 | MATERIALS AND METHODS

2.1 | HEK293 *SCN8A* cell line generation

The wild-type h*SCN8A* gene was polymerase chain reaction (PCR) amplified from human dorsal root ganglion and cloned into a mammalian expression retroviral vector under a cytomegalovirus promoter. The h*SCN8A* R1872Q variant (g5615a; CGG to CAG) was generated by site-directed mutagenesis (QuikChange II Site-Directed Mutagenesis kit; Agilent Technologies, Santa Clara, CA, USA). Plasmids containing wild-type *SCN8A* were used to establish a pool of control cells. Each stable pool was maintained in growth media containing 400 μg/mL G418 for selection. A clonal cell line expressing either wild-type *SCN8A* or R1872Q *SCN8A* was selected from dilution cloning and prioritized by functional sodium current amplitude using the IonWorks

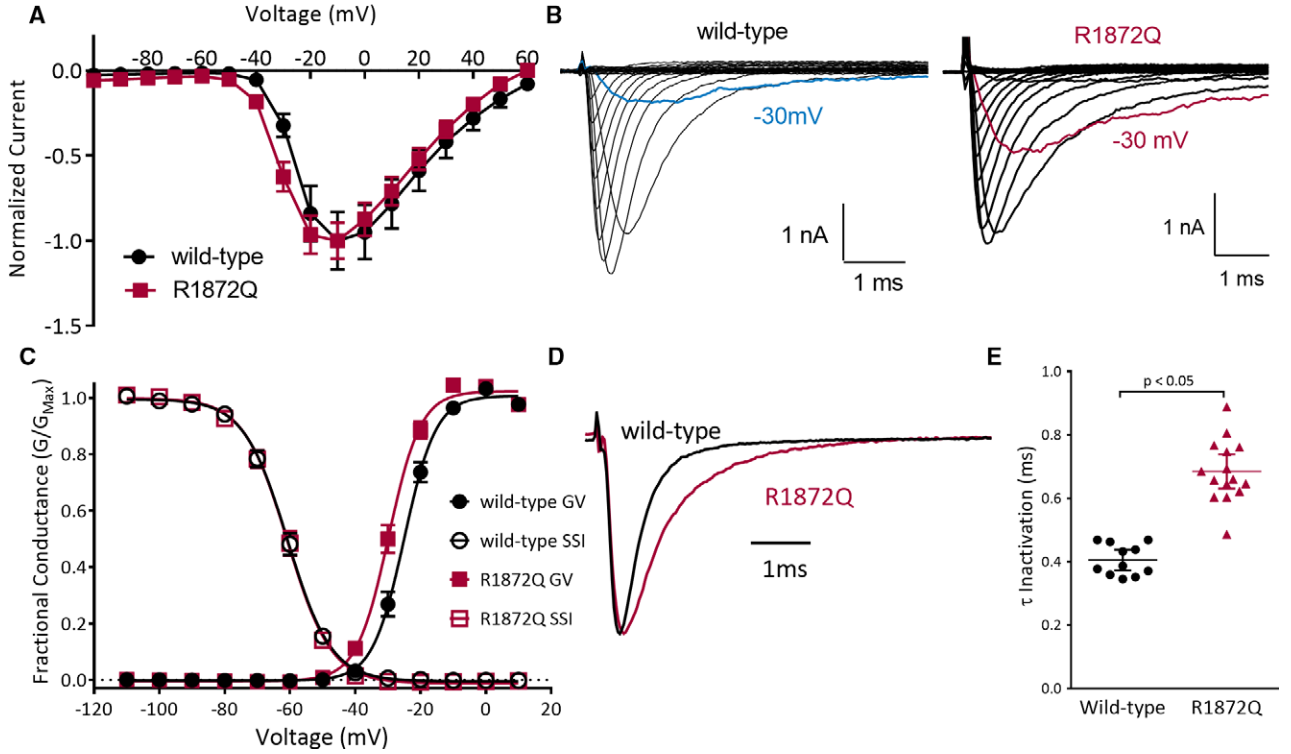

FIGURE 1 *SCN8A* R1872Q characterization. A, Normalized peak current-voltage relationships of $Na_v1.6$ wild-type (black) and $Na_v1.6$ R1872Q (red) channels (n = 10). B, Representative sodium current traces in cells expressing $Na_v1.6$ wild-type or $Na_v1.6$ R1872Q channels; traces at −30 mV are shown in blue and red, respectively. C, Conductance-voltage (GV) relationship for channel activation; $V_{1/2}$ is −25.6 mV for $Na_v1.6$ wild-type and −30.3 mV for $Na_v1.6$ R1872Q (difference of 4.7 mV, n = 10, $P < .05$). Overlap of GV and steady-state inactivation (SSI) curves for $Na_v1.6$ R1872Q (red) and $Na_v1.6$ wild-type (black) channels demonstrates that the $Na_v1.6$ R1872Q variant displays an expanded window current. D, Representative comparative traces illustrating slower inactivation of the $Na_v1.6$ R1872Q channel at a test potential of 0 mV. E, Scatter plots with mean ± standard error of the mean for time constants of inactivation showing that the rate of inactivation is significantly slower in the $Na_v1.6$ R1872Q variant than $Na_v1.6$ wild-type (n = 11-15, $P < .05$)

high-throughput electrophysiology platform (Molecular Devices, Sunnyvale, CA, USA). HEK293 cells expressing either wild-type or R1872Q *SCN8A* were cultured in Dulbecco modified Eagle medium/high glucose containing 10% fetal bovine serum, 2 mmol·L^{-1} sodium pyruvate, 10 mmol·L^{-1} hydroxyethylpiperazine ethane sulfonic acid (HEPES), and 400 μg/mL G418 at 37°C in the presence of 10% CO_2. Cells were routinely passaged every 3-5 days to maintain <80% confluency. All studies were completed within cell passages 7-9.

2.2 | Quantitative PCR methods

Total RNA was isolated from 1 × 10^6 cells for each cell line (RNeasy kit 74106; Qiagen, Hilden, Germany). Residual genomic DNA was eliminated by treating RNA with DNase I (Ambion DNA-free kit AM1906; Thermo Fisher Scientific, Waltham, MA, USA). Quantitative real-time PCR was performed in triplicate using 100 μg total RNA per 20 μL reaction (Taqman One-Step RT-PCR kit 4309169 and ABI Prism 7900HT instrument, Thermo Fisher Scientific). Primer/probe sets used were specific for either human *SCN8A* or human *GAPDH* (reference gene). Relative quantification ($2^{-\Delta\Delta CT}$) was used to compare human *SCN8A* gene expression among the *SCN8A* cell lines relative to HEK293 (each cell line was normalized to endogenous *GAPDH*).

2.3 | PatchXpress protocol and analysis to determine voltage-dependent properties

Whole cell patch clamp biophysical experiments were performed using the PatchXpress 7000A automated patch clamp system (Molecular Devices). The biophysical properties of *SCN8A* R1872Q were compared to wild-type *SCN8A*. Experiments were conducted across multiple days. Test groups (wild-type or mutant cells) were alternated within a single testing day to help control for assay drift. Upon reaching stable whole cell configuration, cells were held at a membrane potential of −120 mV, then depolarized in 10-mV increments from −120 mV to +60 mV. Each depolarizing step was applied for 500 milliseconds followed by a 20-millisecond step at 0 mV. The extracellular recording solution composition was (in mmol·L^{-1}): 135

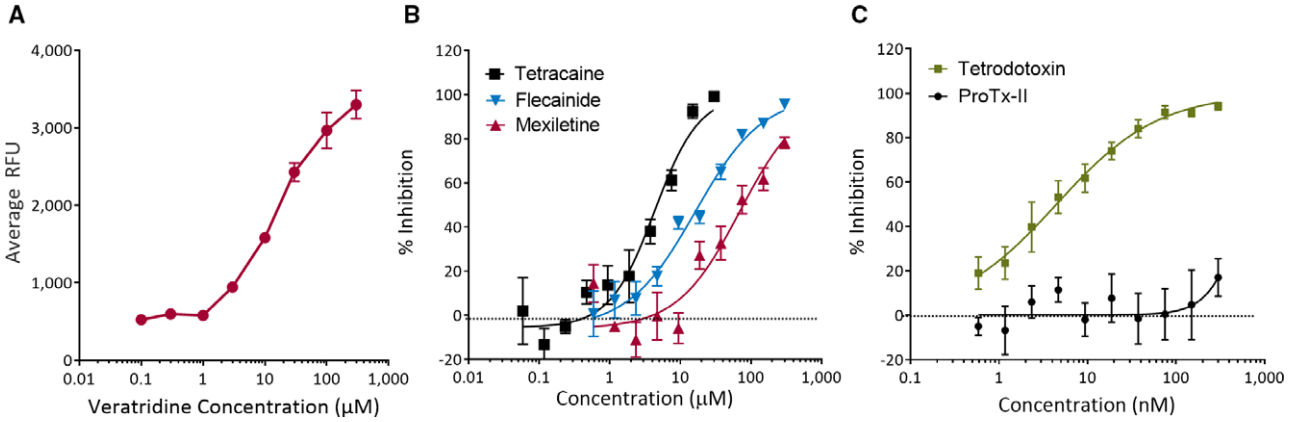

FIGURE 2 Validation of the *SCN8A* R1872Q-containing cell line in a fluorescence-based Na^+ flux assay. A, Veratridine-stimulated, concentration-dependent increase in Na^+ fluorescence in $Na_v1.6$ R1872Q-expressing HEK293 cells. Cells were loaded with 4 μmol·L^{-1} ANG-2 and stimulated with increasing concentrations of veratridine (mean ± standard error of the mean [SEM], n = 4). B, Ten-point concentration response curve (CRC) of traditional small molecule sodium channel blockers against a background of 100 μmol·L^{-1} veratridine in the $Na_v1.6$ R1872Q cell line. Concentration-dependent inhibition was observed for tetracaine, flecainide, and mexiletine (mean ± SEM, n = 4). C, Ten-point CRC of 2 known sodium channel toxins in the presence of 100 μmol·L^{-1} veratridine using the $Na_v1.6$ R1872Q cell line. Concentration-dependent inhibition was observed for tetrodotoxin in the nmol·L^{-1} range, whereas ProTx-II, a $Na_v1.7$ selective toxin, demonstrated minimal inhibitory activity and only at 300 μmol·L^{-1}, the highest concentration tested (mean ± SEM, n = 4). RFU, relative fluorescence units

NaCl, 5.4 KCl, 1 $MgCl_2$, 2 $CaCl_2$, 10 HEPES, 5 glucose, pH 7.4 (300 mOsm). The intracellular solution consisted of (in mmol·L^{-1}): 135 CsF, 10 CsCl, 5 NaCl, 10 HEPES, 5 ethyleneglycoltetraacetic acid, pH 7.3 (290 mOsm).

The peak currents elicited by the Δ10-mV steps (500 milliseconds each) were used to calculate current-voltage relationships. To derive the conductance-voltage (GV) relationship, the calculated reversal potential of +72 mV was used such that conductance = current / (test potential − reversal potential). The peak currents from the second 0-mV (20 milliseconds) step were used to determine voltage-dependent properties of steady-state inactivation (SSI) by plotting as a function of the Δ10-mV (500 milliseconds) prepulse voltage. Both GV and SSI curves were individually fit in GraphPad Prism 6 (GraphPad Software Inc., La Jolla, CA, USA) to the Boltzmann equation to derive the voltage at which 50% of the channels are in the inactivated state ($V_{1/2}$). Individual relationships were normalized such that fractional current = current amplitude/(fitted E_{max} − fitted E_{min}). These normalized data were averaged, plotted as mean ± standard error of the mean values, and fit to the Boltzmann equation to yield 95% confidence intervals in addition to $V_{1/2}$, slope, minimum, and maximum. Nonnormalized amplitudes were comparable between *SCN8A* wild-type and R1872Q clones.

2.4 | Compounds and reagents for FLIPR high-throughput screening

A library of 1320 small molecules was used for high-throughput screening (HTS). Most of the drugs were taken from the Prestwick Chemical Library (Strasbourg-Illkirch, France), a collection of 1280 molecules comprised mostly of drugs approved by the FDA, European Medicines Evaluation Agency, and/or other agencies; additional compounds included sodium channel inhibitors and antiepileptic drugs (AEDs). The drug library was prepared as 10 mmol·L^{-1} stocks in 100% dimethyl sulfoxide (DMSO) and diluted for use at 10 μmol·L^{-1}. Compounds were compressed from 96-well microplates into 384-well Echo LDV plates (Labcyte, San Jose, CA, USA). Lead compounds were obtained from independent suppliers and further characterized with concentration-response curves (CRCs) by adding 15 μL of 10 mmol·L^{-1} compound stocks to 35 μL of DMSO. Serial dilutions were performed by transferring 25 μL of top compound concentration to 25 μL of DMSO and mixed. Dilutions were continued to generate a 10-point CRC. For AEDs and sodium channel inhibitors, 100 mmol·L^{-1} compounds stocks were diluted for use at 300 μmol·L^{-1} and serial dilutions were performed; the final DMSO concentration was 0.3%.

2.5 | FLIPR experiments

The day prior to screening, cells were harvested in growth media and plated on poly-D-lysine-coated, black-walled 384-well microplates with clear bottoms (Greiner Bio-One, Kremsmünster, Austria); 25 μL of a 0.9 × 10^6 cells per mL suspension were seeded into the plates. Plates were incubated at 37°C, 10% CO_2 overnight until used. Prior to testing, growth media were removed from the plate and

10 μL of 4 μmol·L^{-1} Asante NaTRIUM Green-2 (ANG-2; TEFLabs, Austin, TX, USA) was added (mixed with equal volume of 20% Pluronic F127). Cells were protected from light and incubated for 60-90 minutes at room temperature. After incubation, the dye was removed from the plates and replaced with 10 μl (in mM): 135 NaCl, 5.4 KCl, 1 $MgCl_2$, 2 $CaCl_2$, 10 HEPES, 5 Glucose, pH 7.4 (300 mOsm). Cell and assay plates were loaded onto the FLIPR High-Throughput Cellular Screening System (Molecular Devices) and the 5_min_5_min 384 protocol was run, as follows. Ten microliters of a preincubation plate containing EBSS + valinomycin either with or without test compound was added to the cells. Images were taken for 5 minutes to monitor effects on basal Na^+ fluorescence. After the 5-minute incubation, 20 μL of EBSS + 30 μmol·L^{-1} veratridine (with or without test compounds) was added and fluorescence responses were monitored for an additional 5 minutes. Data were exported as maximum-minimum over the 5-minute veratridine addition.

2.6 | PatchXpress protocol to assess pharmacological activity

Wild-type and mutant *SCN8A* cell lines were voltage-clamped at a holding potential of −120 mV to maintain sodium channels in a closed resting state. After current amplitude became stable, the midpoint voltage of SSI was determined for each cell using a series of 5-second conditioning steps to increasingly depolarized voltages (−120 to −40 mV) that preceded a 20-millisecond test pulse to 0 mV to establish magnitude of inactivation. The holding command potential was then set to voltage at which 50% of the channels were in the inactivated state ($V_{1/2}$ - set automatically via PatchXpress scripts). From this holding potential, a 2-millisecond voltage step to holding potential followed by a 20-millisecond depolarizing step to 0 mV and then 2 seconds at the holding potential were applied at a frequency of 0.1 Hz until current amplitude was steady (automatically determined by PatchXpress scripts), at which time a test compound was added. The effect of test reagents on Na_v current amplitude was monitored using the voltage protocol described above, and washed out after reaching steady-state as determined by PatchXpress stability scripts.

Data were collected on a PatchXpress platform using Patch Commander Software (Molecular Devices), then processed and analyzed using DataXpress 2.0 (Molecular Devices). Percentage inhibition was normalized to the average of the control and washout currents according to the formula: % Inhibition = ([Ctrl + Wash] / 2) − Drug/([Ctrl + Wash] / 2) × 100. Normalized concentration-response relationships were fitted using the XLfit software (ID Business Solutions, Guildford, UK) 4-Parameter Logistic Model. Inhibition = $A + ([B - A] / [1 + ([C / x] \text{ ^ } D)])$, where $A = \text{assay}_{min}$ (fixed at 0%), $B = \text{assay}_{max}$ (fixed at 100%), $C = IC_{50}$, and D = slope.

3 | RESULTS

3.1 | Clinical description and variant identification

The patient (female, 11 years old) was diagnosed with epilepsy and global developmental delay consistent with type 13 early infantile epileptic encephalopathy (EIEE13). She is nonverbal. The patient can walk <10 feet with assistance and ankle-foot orthoses. Her first afebrile seizure occurred at 3 months. Seizure types in the past have included atypical absence, myoclonic, tonic, and tonic–clonic head drops. The epilepsy was resistant to more than 10 AEDs and several immunomodulatory therapies, but did respond to carbamazepine.

When the child was 8 years old, a medical laboratory with clinical pathology accreditation (London, UK) identified the presence of a heterozygous c.5615G>A; p.R1872Q *SCN8A* variant in the patient's DNA through next generation sequencing of 66 genes associated with severe developmental delay; the result was confirmed by Sanger sequence analysis. Parental analysis of lymphocyte DNA did not identify the mutation, consistent with a de novo origin in the child. The R1872Q mutation encoded by the *SCN8A* gene was classified as pathogenic with reference to a previous report that identified a different mutation in the *SCN8A* gene (L1290V) associated with epileptic encephalopathy.[10] Subsequently, Wagnon et al[9] reported on a male patient with the identical R1872Q *SCN8A* mutation that was associated with EIEE13.

3.2 | Generation and characterization of the wild-type and $Na_v1.6$ R1872Q variant cell lines

To assess the mutation in a cellular model that would be amenable to HTS, we used the HEK293 cell line, an immortalized human cell line utilized extensively for ion channel physiology experiments and HTS studies.[11] We used site-directed mutagenesis to introduce the R1872Q variant (g5615a; CGG to CAG) into the *SCN8A* cDNA, and then transfected a plasmid containing the mutated cDNA into HEK293 cells and generated a stable clonal $Na_v1.6$ R1872Q cell line. Sequence integrity of the expressed construct in each cell line was confirmed using reverse transcriptase (RT)-PCR and sequencing of the resulting cDNA. A wild-type *SCN8A* stable clonal cell line was also generated for control purposes.

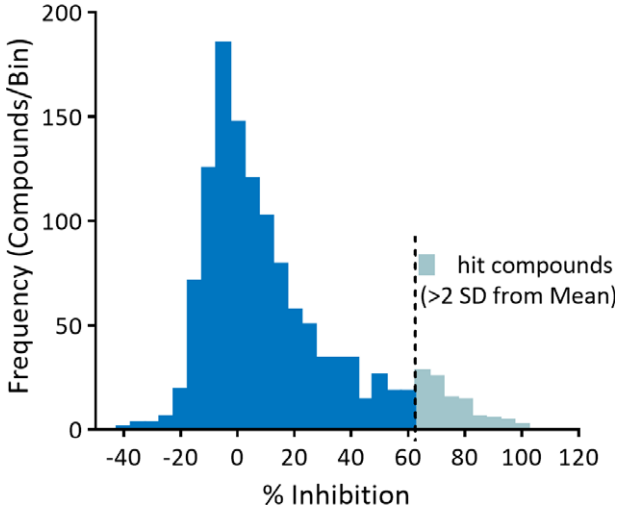

FIGURE 3 Screening results from the 1320-compound library for inhibitory activity against the R1872Q *SCN8A* sodium channel. The histogram shows the number of screened drugs at each given level of inhibition (5%/bin). The bins in light blue represent compounds with inhibitory activity > 2 standard deviations (SD; ≥63.0%) above the group mean (10.8%). A total of 90 compounds met or exceeded this level of inhibitory activity and were defined as hits in the assay. See Table 1 for a complete list of compounds and activity

We then functionally characterized and compared the $Na_v1.6$ R1872Q variant and $Na_v1.6$ wild-type cell lines using electrophysiology. Current-voltage plots were obtained by applying test pulses at membrane potentials between −100 mV and +60 mV (Figure 1A,B). The fractional GV relationship for $Na_v1.6$ R1872Q channel activation revealed a significant 4.7 mV leftward shift in $V_{1/2}$ compared to wild-type channels (−30.3 ± 0.7 mV, n = 10 for $Na_v1.6$ R1872Q and −25.6 ± 0.7 mV, n = 12 for $Na_v1.6$ wild-type, $P < .05$; Figure 1C). These data confirm findings from prior studies on the same mutation.[9] We also investigated the voltage dependence of steady-state inactivation, finding no significant difference between cells bearing mutant or wild-type channels (Figure 1C). There was a small increase in the window current largely due to the leftward shift in voltage dependent activation as noted above (Figure 1C).

Inactivation kinetics were studied at a test potential of 0 mV (Figure 1D). The decay phase was best fit by a single exponential. A significantly delayed rate of inactivation was found in $Na_v1.6$ R1872Q channels compared with $Na_v1.6$ wild-type channels ($P < .05$; Figure 1D). The measured time constant for inactivation was significantly slower for the $Na_v1.6$ R1872Q variant than the wild-type (τ inactivation: 0.7 ± 0.1 milliseconds, n = 15 for R1872Q and 0.4 ± 0.05 milliseconds, n = 11 for wild-type, $P < .05$; Figure 1E). We did not see an elevated persistent

TABLE 1 High-throughput screening results: compounds with significant inhibitory activity against *SCN8A* sodium channels at 10 μmol·L^{-1}

Chemical name	Inhibition, %
Dibucaine	97.8
Methyl benzethonium chloride	97.7
Darifenacin hydrobromide	95.3
Dimethisoquin hydrochloride	93.5
Cloperastine hydrochloride	93.4
Prenylamine lactate	92.6
Fendiline hydrochloride	92.5
Bromperidol	90.6
Carvedilol	89.0
Bepridil hydrochloride	88.9
Naftopidil dihydrochloride	88.6
DO 897/99/BP897	85.6
Proparacaine hydrochloride	85.5
Loperamide hydrochloride	85.4
Nilvadipine	84.9
Dyclonine hydrochloride	83.5
Trihexyphenidyl-D,L hydrochloride	83.3
GBR 12909 dihydrochloride	82.7
Drofenine hydrochloride	81.5
Racecadotril	81.5
Lidoflazine	81.4
Deptropine citrate	78.8
Clomipramine hydrochloride	77.8
Flavoxate hydrochloride	77.5
Alverine citrate salt	77.5
Propafenone hydrochloride	76.8
Trimipramine maleate salt	76.6
Trimebutine	76.5
Droperidol	76.3
Nefazodone hydrochloride	76.2
Ethaverine hydrochloride	75.9
Clemastine fumarate	75.8
Terfenadine	75.6
Mebeverine hydrochloride	75.5
Azelastine hydrochloride	75.4
Metergoline	75.2
Enilconazole	74.7
Progesterone	74.4
Promazine hydrochloride	74.1
Proadifen hydrochloride	74.0
Oxethazaine	73.9

(Continues)

TABLE 1 *(Continued)*

Chemical name	Inhibition, %
Tetracaine hydrochloride	73.6
Thioridazine hydrochloride	73.3
Clemizole hydrochloride	73.2
Ritonavir	72.8
Dicyclomine hydrochloride	71.8
Penbutolol sulfate	71.6
Ethopropazine hydrochloride	71.4
Amitriptyline hydrochloride	71.2
Benfluorex	70.9
(R)-Duloxetine hydrochloride	70.7
Verapamil hydrochloride	70.3
Fluvoxamine maleate	70.0
Homochlorcyclizine dihydrochloride	69.8
Cyclobenzaprine hydrochloride	69.7
Triflupromazine hydrochloride	69.6
Butacaine	69.4
Fluoxetine hydrochloride	69.0
Cyproheptadine hydrochloride	68.8
Spiperone	68.3
Metixene hydrochloride	68.2
Perhexiline maleate	68.1
Benoxinate hydrochloride	67.8
Dilazep dihydrochloride	67.7
Imipramine hydrochloride	67.6
Pergolide mesylate	67.4
Benperidol	67.1
Indatraline hydrochloride	67.0
Econazole nitrate	66.7
Chloropyramine hydrochloride	66.6
Benzonatate	66.6
Dydrogesterone	66.2
Perphenazine	66.1
Mebhydrolin 1,5-naphtalenedisulfonate	65.8
Nafronyl oxalate	65.7
Trimeprazine tartrate	65.6
Flunarizine dihydrochloride	65.5
Nicergoline	65.3
Melengestrol acetate	65.0
Perospirone	64.8
Pizotifen malate	64.8
Moricizine hydrochloride	64.3
Biperiden hydrochloride	64.2
Atomoxetine hydrochloride	64.0
Fipexide hydrochloride	63.7
Benztropine mesylate	63.6
Oxiconazole nitrate	63.6
Paroxetine hydrochloride	63.5
Fluphenazine dihydrochloride	63.3
Diperodon hydrochloride	63.0

(Continues)

TABLE 1 *(Continued)*

List of compounds with significant inhibitory activity at the R1872Q *SCN8A* sodium channel. The 90 compounds listed in the table demonstrated inhibitory activity > 2 standard deviations (≥63.0%) above the mean inhibitory activity of all compounds (10.8%). Data reflect the average of duplicate measures for each compound.

current at a test potential of 0 mV in the $Na_v1.6$ R1872Q line. These data also confirm findings from previous studies.[9]

3.3 | Screening of a library of approved drugs

We utilized a stimulus-activated, fluorescence-based Na^+ flux assay with an FLIPR high-throughput cellular screening system.[11] Fluorescence-based screening assays are frequently used for assessing ion channel function.[12,13] After preincubation with the Na^+ indicator dye, ANG-2, clonal cell lines were tested for their abilities to generate a fluorescent readout in response to veratridine, a neurotoxin that causes persistent opening of sodium channels. Veratridine CRCs were generated using the $Na_v1.6$ R1872Q clonal cell line, revealing a robust dynamic range (Figure 2A) consistent with historical data generated on wild-type $Na_v1.6$ channels and suitable for screening.[14] The ability to detect a concentration-dependent reduction in sodium flux was demonstrated using known sodium channel inhibitors including tetracaine, flecainide, and mexiletine (Figure 2B). The pharmacology of expressed $Na_v1.6$ sodium channels toward channel-specific inhibitors was also evaluated. Cells demonstrated sensitivity to tetrodotoxin, which inhibits voltage-gated sodium channels except $Na_v1.5$, $Na_v1.8$, and $Na_v1.9$, and lack of activity of the tarantula venom peptide, ProTx-II, which is a selective inhibitor of $Na_v1.7$ channels (Figure 2C).[15]

We then initiated screening of a library of 1320 pharmacologically diverse drugs (including the Prestwick Chemical Library of 1280 compounds) at 10-$\mu mol \cdot L^{-1}$ concentration; compounds were evaluated in duplicate. A set concentration of 10 $\mu mol \cdot L^{-1}$ was considered to be suitable to identify compounds with a level of potency and effectiveness in the in vitro screen that might translate to pharmacological activity in vivo. Z-prime values were >0.5, signifying a robust,

TABLE 2 Characterization of known antiepileptic drugs against wild-type and R1872Q *SCN8A* cell lines

Compound name	*SCN8A* R1872Q maximum inhibition, %	Wild-type *SCN8A* maximum inhibition, %	*SCN8A* R1872Q average IC_{50}, μmol·L^{-1}	Wild-type *SCN8A* average IC_{50}, μmol·L^{-1}
Clonazepam	96.6	102.2	39.8	22.6
Tiagabine	80.6	94.2	71.8	31.1
Clobazam	73.1	83.7	137.7	89.2
Retigabine	67.0	82.4	133.2	62.3
Phenytoin	60.6	80.7	119.0	55.9
Carbamazepine	60.0	70.4	228.4	153.2
Lamotrigine	36.8	69.8	>300	179.8
Eslicarbazepine acetate	28.8	41.7	>300	>300
Oxcarbazepine	26.7	46.7	>300	261.2
Ethotoin	20.1	20.5	>300	300.0
Felbamate	19.8	30.2	>300	247.0
Ethosuximide	18.8	12.1	>300	>300
Methsuximide	18.1	31.5	>300	>300
Phenobarbital	18.0	31.1	>300	>300
Vigabatrin	16.2	10.4	>300	>300
Levetiracetam	15.2	13.4	>300	>300
Lacosamide	14.3	8.3	>300	>300
Topiramate	11.9	12.9	>300	>300
Divalproex sodium	11.8	14.4	>300	>300
Gabapentin	11.5	7.2	>300	>300
Rufinamide	10.5	3.0	>300	>300
Primidone	8.3	8.0	>300	>300
Valproic acid	5.7	6.2	>300	>300
Zonisamide	−0.4	6.8	>300	>300

Characterization of known antiepileptic drugs against wild-type and $Na_v1.6$ R1872Q *SCN8A* cell lines. Data are based on 10-point concentration-response curves, 10 nmol·L^{-1} to 300 μmol·L^{-1}, n = 4 across 2 separate trials in the presence of 30 μmol·L^{-1} veratridine. Percentage inhibition is normalized to 30 μmol·L^{-1} tetracaine (100%) and dimethyl sulfoxide controls (0%).

high-throughput assay suitable for screening of the $Na_v1.6$ R1872Q cell line to identify inhibitors of sodium influx. Screening was conducted against a background of 30 μmol·L^{-1} veratridine and normalized to 30 μmol·L^{-1} tetracaine (100%) and DMSO (0%) controls. The average inhibition for the entire library was 10.8%. Ninety compounds showed >2 standard deviation inhibition (≥63.0%) from the mean (Figure 3A); the majority of these have not been previously linked to sodium channels, in particular with activity against $Na_v1.6$, or other ion channel activity in general. This group of 90 compounds was then screened a second time using independently sourced drugs at 10 μmol·L^{-1} to confirm activity in the assay. The complete list of 90 hit compounds along with inhibitory activity is shown in Table 1.

3.4 | Comparison to traditional pharmacological agents

We sought to further assess the response of both the $Na_v1.6$ R1872Q and $Na_v1.6$ wild-type lines to 24 AEDs using CRCs (10 points, 10 nmol·L^{-1} to 300 μmol·L^{-1}, n = 4 across 2 separate trials). Drugs were tested in both the $Na_v1.6$ R1872Q and wild-type $Na_v1.6$ cellular models. Across a full CRC, several AEDs showed strong inhibition of both channels (eg, clonazepam), whereas the majority were far less effective, even at relatively high drug concentrations of 300 μmol·L^{-1} (Table 2). We also generated CRCs for 10 known sodium channel inhibitors in wild-type and $Na_v1.6$ R1872Q cell lines. Most compounds demonstrated a moderate level of activity with a trend for greater

TABLE 3 Characterization of known sodium channel inhibitors for selectivity to $Na_v1.6$ R1872Q

Compound name	*SCN8A* R1872Q maximum inhibition, %	Wild-type *SCN8A* maximum inhibition, %	*SCN8A* R1872Q average IC_{50}, $\mu mol \cdot L^{-1}$	Wild-type *SCN8A* average IC_{50}, $\mu mol \cdot L^{-1}$	Indicated therapeutic class
Mexiletine hydrochloride	68.6	84.9	119.6	53.1	Antiarrhythmic
Disopyramide	68.0	72.9	150.0	84.4	Antiarrhythmic
Carbamazepine	60.0	70.4	228.4	153.2	Analgesic/ anticonvulsant
Prilocaine hydrochloride	46.9	57.9	299.7	174.8	Anesthetic
Articaine hydrochloride	40.5	60.2	>300	153.4	Anesthetic
Procaine hydrochloride	28.1	34.6	>300	>300	Anesthetic
Oxcarbazepine	26.7	46.7	>300	261.2	Anticonvulsant
Benzocaine	24.3	42.3	>300	279.2	Anesthetic
Topiramate	11.9	12.9	>300	>300	Anticonvulsant
Tocainide hydrochloride	9.4	15.1	>300	>300	Anesthetic

Data acquired by 10-point concentration-response curves from 10 $nmol \cdot L^{-1}$ to 300 $\mu mol \cdot L^{-1}$, n = 4 across 2 separate trials, in the presence of 30 $\mu mol \cdot L^{-1}$ veratridine. Percentage inhibition is normalized to 30 $\mu mol \cdot L^{-1}$ tetracaine (100%) and dimethyl sulfoxide controls (0%).

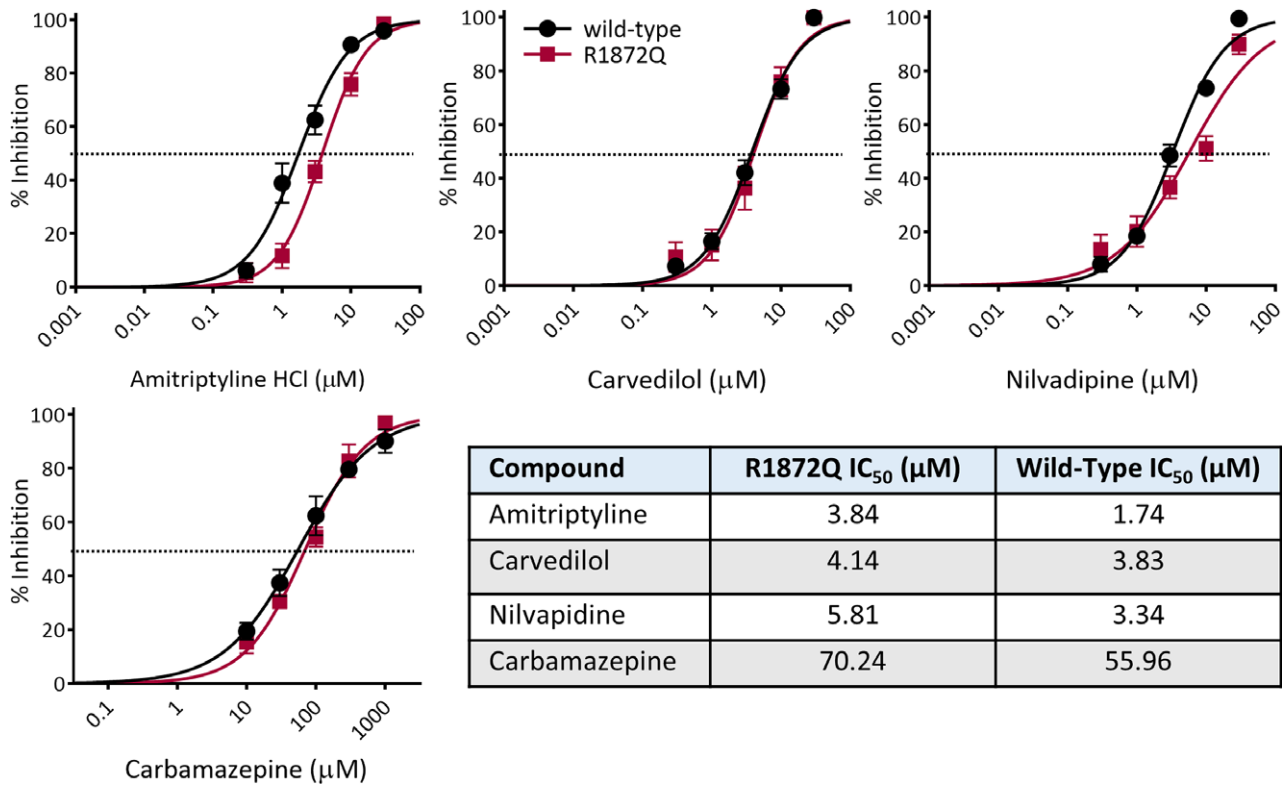

Compound	R1872Q IC_{50} (μM)	Wild-Type IC_{50} (μM)
Amitriptyline	3.84	1.74
Carvedilol	4.14	3.83
Nilvapidine	5.81	3.34
Carbamazepine	70.24	55.96

FIGURE 4 Electrophysiological characterization of lead compounds. Graphs show concentration-dependent current inhibition (%) of $Na_v1.6$ wild-type (black circles) and $Na_v1.6$ R1872Q (red squares) channels for amitriptyline, carvedilol, nilvadipine, and carbamazepine. Five-point concentration-response curves ($n \geq 4$ for each data point) were generated for all 4 test compounds on wild-type and $Na_v1.6$ R1872Q variants. Table shows the fitted mean IC_{50} for each compound against both cell lines

inhibitory potency on the $Na_v1.6$ wild-type cell line compared to the $Na_v1.6$ R1872Q cell line (Table 3).

3.5 | Electrophysiological evaluation of select compounds

To further explore the activity of compounds that demonstrated strong inhibitory effects in the FLIPR screen, we evaluated 3 lead compounds, amitriptyline, carvedilol, and nilvadipine, in an electrophysiological assay, along with carbamazepine; a well-known sodium channel blocker and an AED with demonstrated clinical benefit in the *SCN8A* R1872Q patient. The inhibitory effect of these compounds was assessed using the PatchXpress automated electrophysiological platform, with $Na_v1.6$ R1872Q and wild-type cell lines held at the midpoint voltage of SSI. Peak currents in response to a depolarizing pulse were measured across a 5-point CRC, which confirmed a strong inhibitory effect of the test compounds in a concentration-dependent manner (Figure 4). The IC_{50} values for $Na_v1.6$ wild-type and $Na_v1.6$ R1872Q were determined from the CRCs and showed the same trend for greater potency of effect on the wild-type over mutant channel as was noted above with AEDs (Table 2) and sodium channel inhibitors (Table 3).

4 | DISCUSSION

Our study confirms the utility of a high-throughput functional assay to comprehensively evaluate approved medicines to identify potential targeted treatments that could be available for immediate clinical use. This work shows that at least for a sodium channel with a clear gain-of-function mutation, a comprehensive drug repurposing screen is both feasible and effective. The present study suggests that testing only one or a few candidate drugs to identify a potential repurposed treatment for a genetic condition provides too limited a picture of the potential drug opportunities that could be therapeutically evaluated.

When translating findings from cellular assays to therapeutic use, it is essential to consider whether concentrations required for in vitro activity are physiologically relevant to prescribed clinical doses. To that end, we compared the drug concentrations of our lead compounds, amitriptyline, nilvadipine, and carvedilol, as well as carbamazepine, required to inhibit $Na_v1.6$ R1872Q sodium channel activity in vitro, to published data on CNS drug concentrations from standard oral clinical doses. Carbamazepine has an average brain concentration of 3.52 $\mu mol \cdot L^{-1}$ over a variety of doses when unbound fraction and brain penetrance are taken into account.[16,17] Relating that CNS level to the data generated with our electrophysiological evaluation (Figure 4) correlates to 4.7% inhibition against the $Na_v1.6$ R1872Q channel and 9.6% inhibition against the wild-type ion channel with clinical doses. When carvedilol is taken at a 100-mg daily dose (50 mg, twice daily), a steady-state maximum plasma concentration of 205 ng/mL (0.50 $\mu mol \cdot L^{-1}$) is reached within 1.5 hours.[18] Carvedilol penetrates the blood-brain barrier, resulting in an estimated average CNS concentration of 0.15 $\mu mol \cdot L^{-1}$.[19] The steady-state free brain concentrations would therefore correspond to an inhibition of 5.6% and 7.4% against the mutant and the wild-type channels, respectively, which is similar to carbamazepine. Likewise, nilvadipine, a calcium blocker used to treat hypertension, reaches a steady-state maximum plasma concentration of 11.7 ng/mL with 16 mg taken daily.[20] The concentration that reaches the brain, roughly 0.05 $\mu mol \cdot L^{-1}$,[21] would correspond to 1.3% inhibition against the mutant and 0.4% against the wild-type according to the CRCs, which is lower than predicted values for carbamazepine. Amitriptyline is an effective antidepressant at steady-state plasma concentrations at 150-250 ng/mL.[22] Although data on brain levels of amitriptyline following chronic dosing are somewhat limited, studies in rodents suggests levels can reach 5-7 $\mu mol \cdot L^{-1}$.[23] From the present study, amitriptyline at this concentration would correspond to a 59% to 84% inhibition of $Na_v1.6$ channels based on results from the electrophysiological assay (Figure 4).

Whereas nilvadipine has not been previously reported to act on sodium channels, both amitriptyline and carvedilol are known to inhibit sodium channels in a use-dependent manner.[24,25] Amitriptyline has high affinity for both open and inactivated channels, but low affinity for resting state channels.[26] Binding to the open and inactivated channel states is also a common feature of AEDs,[27] allowing for preferential inhibition of high-frequency repetitive firing neurons during seizures with more limited impact on normal brain activity.[28] Precise mechanisms of binding and how these 3 inhibitors affect the $Na_v1.6$ contribution to resurgent and persistent sodium-derived currents in neurons remain to be investigated.[6,7] Nevertheless, this work identified interesting drug candidates for further investigation, especially amitriptyline, which was shown to be a potent inhibitor of $Na_v1.6$. Although the way *SCN8A* mutations cause disease in vivo cannot be fully captured in an in vitro heterologous expression system, the active compounds we identified through HTS represent important candidates for further characterization in appropriate in vivo models, and for subsequent design of new chemical entities.

Identifying viable candidates from an extensive library of clinically approved drugs that directly inhibit a gain-of-function pathogenic mutation illustrates the feasibility and potential of comprehensive drug repurposing screening to identify new therapeutic options for serious genetic conditions. Comparing estimated CNS exposure at clinically

established doses of a drug with assay inhibitory activity provides an opportunity for more informed selection of therapeutically meaningful treatment decisions in affected patients.

ACKNOWLEDGMENTS

This work was supported by the National Institute of Neurological Disorders and Stroke (U01 NS099705, U01 NS090407, U01 NS090415), National Institute of Mental Health (R01 MH107396, RO1 MH111417), National Institute of Biomedical Imaging and Bioengineering (RO1 EB018308), Centers for Disease Control and Prevention (U48 DP005008-01S4), and Office of Naval Research (N000141310672). The authors would like to thank Zhixin Lin for work on electrophysiology experiments, Michael Andresen for editorial review, and Alissa Dahlke for preparation of the manuscript.

DISCLOSURE OF CONFLICT OF INTEREST

B.C.G., C.M.M., J.R., M.A.F., G.R.S., S.Petrov., O.D., M.M., S.Petrou, and D.B.G. have financial interests in Pairnomix. D.B.G. also has a financial interest in Praxis Pharmaceuticals. S.Petrou also has financial interest in Praxis Pharmaceuticals and receives funding from RogCon. O.D. receives research support from Novartis, PTC Therapeutics, GW Pharmaceuticals, and Zogenix. The remaining authors have no conflicts of interest. We confirm that we have read the Journal's position on issues involved in ethical publication and affirm that this report is consistent with those guidelines.

REFERENCES

1. Melnikova I. Rare diseases and orphan drugs. Nat Rev Drug Discov. 2012;11:267–8.
2. EpiPM Consortium. A roadmap for precision medicine in the epilepsies. Lancet Neurol. 2015;14:1219–28.
3. Caldwell JH, Schaller KL, Lasher RS, et al. Sodium channel Na (v)1.6 is localized at nodes of Ranvier, dendrites, and synapses. Proc Natl Acad Sci U S A. 2000;97:5616–20.
4. Hu W, Tian C, Li T, et al. Distinct contributions of Na(v)1.6 and Na(v)1.2 in action potential initiation and backpropagation. Nat Neurosci. 2009;12:996–1002.
5. Rush AM, Dib-Hajj SD, Waxman SG. Electrophysiological properties of two axonal sodium channels, Nav1.2 and Nav1.6, expressed in mouse spinal sensory neurones. J Physiol. 2005;564:803–15.
6. Raman IM, Sprunger LK, Meisler MH, et al. Altered subthreshold sodium currents and disrupted firing patterns in Purkinje neurons of Scn8a mutant mice. Neuron. 1997;19:881–91.
7. Smith MR, Smith RD, Plummer NW, et al. Functional analysis of the mouse Scn8a sodium channel. J Neurosci. 1998;18:6093–102.
8. Meisler MH, Helman G, Hammer MF, et al. SCN8A encephalopathy: research progress and prospects. Epilepsia. 2016;57:1027–35.
9. Wagnon JL, Barker BS, Hounshell JA, et al. Pathogenic mechanism of recurrent mutations of SCN8A in epileptic encephalopathy. Ann Clin Transl Neurol. 2016;3:114–23.
10. Carvill GL, Heavin SB, Yendle SC, et al. Targeted resequencing in epileptic encephalopathies identifies de novo mutations in CHD2 and SYNGAP1. Nat Genet. 2013;45:825–30.
11. Chen MX, Gatfield K, Ward E, et al. Validation and optimization of novel high-throughput assays for human epithelial sodium channels. J Biomol Screen. 2015;20:242–53.
12. Huang CJ, Harootunian A, Maher MP, et al. Characterization of voltage-gated sodium-channel blockers by electrical stimulation and fluorescence detection of membrane potential. Nat Biotechnol. 2006;24:439–46.
13. Zhao F, Li X, Jin L, et al. Development of a rapid throughput assay for identification of hNav1.7 antagonist using unique efficacious sodium channel agonist, antillatoxin. Mar Drugs. 2016;14:1–12.
14. Zhu HL, Wassall RD, Takai M, et al. Actions of veratridine on tetrodotoxin-sensitive voltage-gated Na currents, Na1.6, in murine vas deferens myocytes. Br J Pharmacol. 2009;157:1483–93.
15. Schmalhofer WA, Calhoun J, Burrows R, et al. ProTx-II, a selective inhibitor of NaV1.7 sodium channels, blocks action potential propagation in nociceptors. Mol Pharmacol. 2008;74:1476–84.
16. Morselli PL, Baruzzi A, Gerna M, et al. Carbamazepine and carbamazepine-10, 11-epoxide concentrations in human brain. Br J Clin Pharmacol. 1977;4:535–40.
17. Riva R, Albani F, Ambrosetto G, et al. Diurnal fluctuations in free and total steady-state plasma levels of carbamazepine and correlation with intermittent side effects. Epilepsia. 1984;25:476–81.
18. Tenero D, Boike S, Boyle D, et al. Steady-state pharmacokinetics of carvedilol and its enantiomers in patients with congestive heart failure. J Clin Pharmacol. 2000;40:844–53.
19. Bart J, Dijkers EC, Wegman TD, et al. New positron emission tomography tracer [(11)C]carvedilol reveals P-glycoprotein modulation kinetics. Br J Pharmacol. 2005;145:1045–51.
20. Rosenthal J. Nilvadipine: profile of a new calcium antagonist. An overview. J Cardiovasc Pharmacol. 1994;24(suppl 2):S92–107.
21. Takakura S, Sogabe K, Satoh H, et al. Nilvadipine as a neuroprotective calcium entry blocker in a rat model of global cerebral ischemia. A comparative study with nicardipine hydrochloride. Neurosci Lett. 1992;141:199–202.
22. Ziegler VE, Co BT, Taylor JR, et al. Amitriptyline plasma levels and therapeutic response. Clin Pharmacol Ther. 1976;19:795–801.
23. Glotzbach RK, Preskorn SH. Brain concentrations of tricyclic antidepressants: single-dose kinetics and relationship to plasma concentrations in chronically dosed rats. Psychopharmacology. 1982;78:25–7.
24. Bankston JR, Kass RS. Molecular determinants of local anesthetic action of beta-blocking drugs: implications for therapeutic management of long QT syndrome variant 3. J Mol Cell Cardiol. 2010;48:246–53.
25. Barber MJ, Starmer CF, Grant AO. Blockade of cardiac sodium channels by amitriptyline and diphenylhydantoin. Evidence for two use-dependent binding sites. Circ Res. 1991;69:677–96.

26. Wang GK, Russell C, Wang SY. State-dependent block of voltage-gated Na+ channels by amitriptyline via the local anesthetic receptor and its implication for neuropathic pain. Pain. 2004;110:166–74.
27. Xie X, Lancaster B, Peakman T, et al. Interaction of the antiepileptic drug lamotrigine with recombinant rat brain type IIA Na+ channels and with native Na+ channels in rat hippocampal neurones. Pflugers Arch. 1995;430:437–46.
28. Rogawski MA, Loscher W. The neurobiology of antiepileptic drugs. Nat Rev Neurosci. 2004;5:553–64.

How to cite this article: Atkin TA, Maher CM, Gerlach AC, et al. A comprehensive approach to identifying repurposed drugs to treat *SCN8A* epilepsy. *Epilepsia*. 2018;00:1–12. https://doi.org/10.1111/epi.14037